HS^- results in a change of only about 20 mV in the corresponding computed Eh in Fig. 2, whereas the total vertical range exceeds 1000 mV. The same argument applies to the computed activity coefficients: any realistic change in activity coefficients results in a trivial change in the distribution of computed Eh values.

The *p*H is important in determining the distribution of points in Fig. 2. In fact, the linear correlation among computed *p*E (negative logarithm of the electron activity) (or Eh) values reported in some publications, for example, (*8*), for coexisting aqueous couples appears to reflect an autocorrelation among the dominant *p*H terms in the Nernst equations for each of the couples.

There are published suggestions that Eh measurements might be improved if the values were computed from analyses of "indicator" couples, such as I^-/IO_3^- (*15*) or As(III)/As(V) (*16*). Unfortunately, this approach does not circumvent the fundamental difficulty that redox reactions in the waters are not at internal equilibrium among themselves. Therefore, an "indicator" Eh no more represents a master redox value for the water than the usual Eh as measured by a noble-metal electrode. Whitfield (*4*) has suggested that Eh measurements may still be useful as qualitative indicators of the overall redox state of a water sample. However, we believe that it would be better to measure certain sensitive species, such as aqueous oxygen, hydrogen sulfide, or methane as qualitative guides to the redox status of the waters.

The concept of Eh remains a valuable tool for theoretical and pedantic purposes. However, in the apparent absence of internal redox equilibrium, investigators should abandon the use of any measured master Eh for predicting the equilibrium chemistry of redox reactions in normal ground waters. Our conclusions are most severe in the context of predictive computer modeling of the chemistry of natural waters and wastewaters. In order to provide meaningful redox input for such models, it may be necessary to analyze the samples for the dominant ions of every redox element of interest. Wolery (*17*) has suggested this approach for testing the state of redox equilibrium, using his EQ3NR computer model. If any measured Eh is used as input for equilibrium calculations, the burden rests with the investigator to demonstrate the reversibility of the system.

RALPH D. LINDBERG
DONALD D. RUNNELLS*
Department of Geological Sciences, University of Colorado, Boulder 80309

References and Notes

1. W. Stumm, *Adv. Water Pollut. Res. (Munic* 283 (1967).
2. J. C. Morris and W. Stumm, in *Equilibrium Concepts in Natural Waters Systems*, W. Stumm, Ed. (American Chemical Society, Washington, D.C., 1967), p. 270.
3. W. Back and I. L. Barnes, *U.S. Geol. Surv. Prof. Pap. 424C* (1961), p. 366; D. Langmuir, in *Procedures in Sedimentary Petrology*, R. E. Carver, Ed. (Wiley-Interscience, New York, 1971), p. 597; K. A. I. Natarajan, thesis, University of Minnesota (1972); T. Frevert, *Arch. Hydrobiol. Suppl.* 55, 278 (1979); R. A. Berner, *J. Sediment. Petrol.* 51, 359 (1981); R. D. Lindberg, thesis, University of Colorado (1983).
4. M. Whitfield, *Limnol. Oceanogr.* 19, 857 (1974).
5. D. K. Nordstrom, E. A. Jenne, J. W. Ball, in *Chemical Modeling in Aqueous Systems*, E. A. Jenne, Ed. (Symposium Series 93, American Chemical Society, Washington, D.C., 1979), p. 51.
6. R. A. Berner, *Geochim. Cosmochim. Acta* 27, 563 (1963); J. Boulegue and G. Michard, in *Chemical Modeling in Aqueous Systems*, E. A. Jenne, Ed. (Symposium Series 93, American Chemical Society, Washington, D.C., 1979), p. 25.
7. O. P. Bricker, *Am. Mineral.* 50, 1296 (1965).
8. D. C. Thorstenson, *Geochim. Cosmochim. Acta* 34, 745 (1970).
9. A. B. Carpenter and R. N. Stoufer, *Influence of Organic Carbon and Microorganisms on Iron and Sulfide Concentrations in Ground Water* (Document PB-270-640, National Technical Information Service, Springfield, Va., 1977).
10. D. K. Nordstrom, thesis, Stanford University (1977); S. Emerson, R. E. Cranston, P. S. Liss, *Deep-Sea Res.* 26, 859 (1979); W. E. Galloway, G. E. Smith, C. L. Ho, J. P. Morton, J. K. Gluck, *Report of Investigations, No. 118* (Bureau of Economic Geology, University of Texas, Austin, 1982).
11. M. D. Edwards, *U.S. Geol. Surv. Open-File Rep. 77-259* (1977).
12. D. D. Runnells and R. D. Lindberg, *J. Geochem. Explor.* 15, 37 (1981).
13. L. N. Plummer *et al.*, *U.S. Geol. Surv. Water-Resources Invest. 76-13* (1976).
14. R. M. Garrels and C. L. Christ, *Solutions, Minerals, and Equilibria* (Freeman, Cooper, San Francisco, 1965).
15. P. S. Liss, J. R. Herring, E. D. Goldberg, *Nature (London) Phys. Sci.* 242, 108 (1973).
16. J. A. Cherry, A. U. Shaikh, D. E. Tallman, R. V. Nicholson, *J. Hydrol.* 43, 373 (1979).
17. T. J. Wolery, *Report No. UCRL-53414* (Lawrence Livermore National Laboratory, Livermore, Calif., 1983).
18. We thank the personnel of the NAWDEX office, Reston, Va., for their assistance. This research was supported by the Rocky Mountain Energy Corporation.
* To whom requests for reprints should be addressed.

6 March 1984; accepted 22 May 1984

Homology of Genome of AIDS-Associated Virus with Genomes of Human T-Cell Leukemia Viruses

Abstract. *A T lymphotropic virus found in patients with the acquired immune deficiency syndrome (AIDS) or lymphadenopathy syndrome has been postulated to be the cause of AIDS. Immunological analysis of this retrovirus and its biological properties suggest that it is a member of the family of human T-lymphotropic retroviruses known as HTLV. Accordingly, it has been named HTLV-III. In the present report it is shown by nucleic acid hybridization that sequences of the genome of HTLV-III are homologous to the structural genes* (gag, pol, *and* env) *of both HTLV-I and HTLV-II and to a potential coding region called pX located between the* env *gene and the long terminal repeating sequence that is unique to the HTLV family of retroviruses.*

Human T-cell leukemia virus (HTLV) was first identified as an infectious agent etiologically associated with adult T-cell leukemia (ATL) (*1*). A related but distinct retrovirus was isolated from a T-cell variant of hairy cell leukemia (*2*). These viruses, known, respectively, as HTLV-I and HTLV-II, show a tropism for human T cells, particularly $OKT4^+$ cells, and have the capacity to immortalize and transform normal T cells in culture (*3*), alter certain T-cell immune functions in vitro (*4*), induce the formation of giant multinucleated T cells (*5*), and, in some cases, selectively kill certain T cells (*6*). These properties and data from epidemiologic studies of the acquired immune deficiency syndrome (AIDS), which is uniformly associated with $OKT4^+$ helper cell depletion (*7*), led us and others to speculate (*8*) that a member of the HTLV family might be the etiological agent of this disease. In support of this hypothesis was the finding that up to 80 percent of AIDS patients, but less than 1 percent of non-AIDS patients from similar risk groups, have serum antibodies that react with the envelope protein of HTLV (*9*). However, actual isolations of the known subgroups of HTLV (that is, HTLV-I and HTLV-II) from AIDS patients were infrequent (*10*).

Recently, we reported repeated isolations of a T lymphotropic retrovirus with cytopathic but not immortalizing activity from patients with AIDS (*11*). This virus can be grown in a previously immortalized T-cell line (HT) that is relatively resistant to the cytopathic effects of the virus and can grow in the absence of T-cell growth factor (interleukin-2) (*12*). Using the infected cells as well as purified virus particles in immunological assays, we found that the serum of 80 to 100 percent of AIDS patients and 70 to 80 percent of patients with lymphadenopathy syndrome reacted positively (*13*). On the basis of its T-cell tropism, the size and Mg^{2+} preference of its reverse transcriptase, the size of its major core protein (24,000 daltons) (*14*), some anti-

genic cross-reactivity of its proteins with HTLV-I and HTLV-II (*14*), and its capacity to induce formation of giant multinucleated cells (*12*), we considered this virus to be a member of the HTLV family and designated it HTLV-III. Here we show that certain sequences of the genome of HTLV-III and both HTLV-I and HTLV-II are homologous, with the most conserved sequences being located within the *gag-pol* region and less but detectable homology occurring in the *env* and pX region.

Virus particles were purified from supernatant fluids of HT cells, clone 9 (H9) infected with HTLV-III (HTLV-III$_B$) by centrifugation through a sucrose density gradient at equilibrium (*12*). HTLV-III$_B$ was originally obtained from pooled supernatants of short-term lymphocyte cultures of AIDS patients. Virus particles were also purified from normal peripheral blood lymphocytes newly infected by virus of a primary leukocyte culture of another AIDS patient (HTLV-III$_Z$) (*11*). The particles were lysed with sodium dodecyl sulfate (SDS), digested with proteinase K, and directly chromatographed on an oligo(dT) cellulose column. The resulting polyadenylate [poly(A)]-containing RNA was used as template to synthesize ^{32}P-labeled complementary DNA (cDNA) in the presence of oligo(dT) primers. The size of the resultant cDNA ranged from 0.1 to 10 kb (not shown). When these labeled cDNA's were hybridized to poly(A)-containing RNA purified from infected and uninfected H9 cells as well as other uninfected human cell lines, only the infected H9 cells contained homologous RNA sequences as evidenced by discrete RNA bands after Northern hybridization. Figure 1 shows that cDNA preparations from HTLV-III$_B$ and HTLV-III$_Z$ gave identical patterns, detecting RNA species of about 9.0, 4.2, and 2.0 kb. These bands are similar in size to those corresponding to genomic size messenger RNA (mRNA) and spliced mRNA's of *env* and pX sequences previously observed in cells infected with HTLV-I (*15*), consistent with the anticipated relatedness of these viruses. Furthermore, viral mRNA bands of HTLV-II–infected cells were detected with an HTLV-III cDNA probe (Fig. 1b, lane 6) and again the sizes of the mRNA were like those with HTLV-I.

To determine directly the homology between HTLV-III and HTLV-I and HTLV-II, we hybridized HTLV-III cDNA to cloned genomes of HTLV-I and HTLV-II digested with specific restriction endonucleases. Complete genomes of a prototype HTLV-I (*16*), an HTLV-I variant called HTLV-Ib (*16*), and HTLV-II were digested with two restriction enzymes as indicated in the

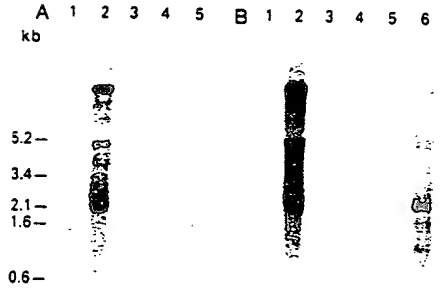

Fig. 1. HTLV-III–specific sequences in cellular RNA from HTLV-infected cells. Poly(A)-selected cellular RNA was size-separated by formaldehyde-agarose gel electrophoresis, transferred to Zeta probe membrane (Bio-Rad Labs) by electroelution and hybridized to (A) HTLV-III$_B$ cDNA and (B) HTLV-III$_Z$ cDNA. (A and B) Lane 1, uninfected H9 cells (5 μg); lane 2, HTLV-III$_B$–infected H9 cells (10 μg); lane 3, leukemic Jurkat cells (10 μg); lane 4, HTLV-I–infected C5/MJ cells (5 μg); and lane 5, HTLV-II–infected MO cells (5 μg). (B) Lane 6, a longer exposure of lane 5 in (B). Poly(A)-selected RNA was prepared by guanidine-HCl extraction and cesium chloride centrifugation followed by oligo(dT) cellulose chromatography as described (*24*). The cDNA was transcribed from poly(A)-selected virus-associated RNA with the use of oligo(dT) as a primer and avian myeloblastosis virus RNA-directed DNA polymerase as described (*25*). The hybridization was performed at 37°C for 16 hours in a mixture containing 40 percent formamide, 5× standard sodium chloride and sodium citrate (SSC; 0.15*M* NaCl and 0.015*M* sodium citrate, *p*H 7), 0.05*M* sodium phosphate buffer (*p*H 7), 5× PM (0.02 percent each of bovine serum albumin, polyvinylpyrrolidone, and Ficoll 400), yeast RNA (200 μg/ml), denatured salmon sperm DNA (20 μg/ml), 0.1 percent SDS, and 10 percent dextran sulfate. The membrane was subsequently repeatedly washed with 2× SSC and 0.1 percent SDS at 62°C, air-dried, and exposed to a Kodak XAR film with the use of intensifying screens.

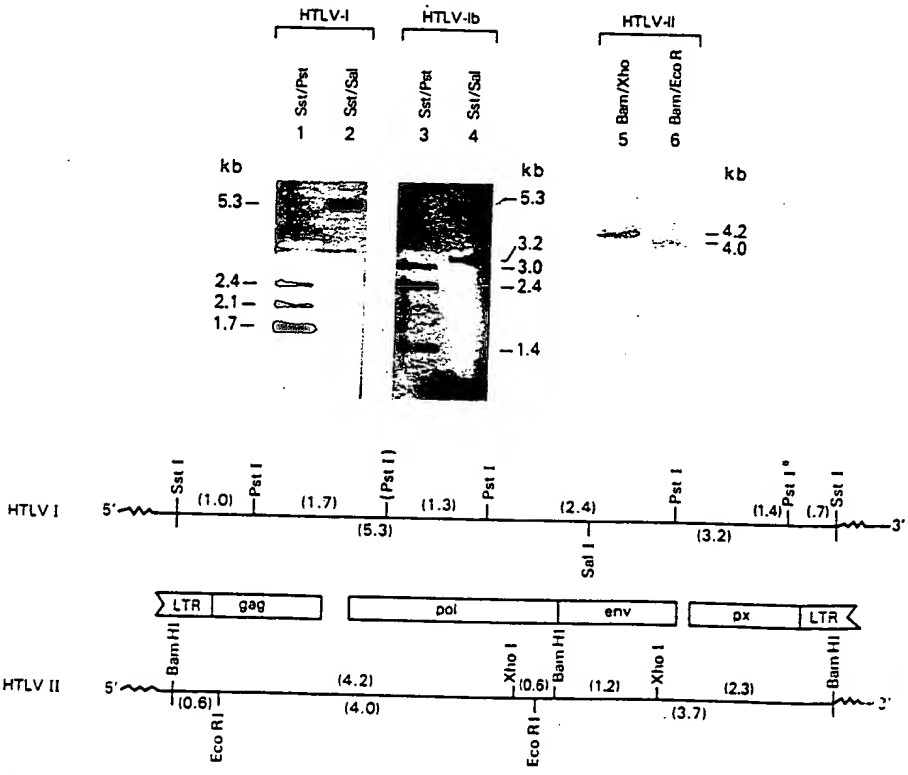

Fig. 2. Relatedness of the genome of HTLV-III$_B$ with the genomes of HTLV-I and HTLV-II. Sites of digestion by the relevant restriction enzymes and the expected sizes of the fragments are shown below the gels. Cloned HTLV-I (λST), HTLV-Ib (λMC), and HTLV-II (pMO) DNA's were digested with the indicated restriction enzymes and fragments were separated by agarose gel electrophoresis, transferred to a nitrocellulose membrane (*23*), and hybridized with HTLV-III$_B$cDNA. Lanes 1 and 2, HTLV-I (λST) DNA digested with Sst I plus Pst I and Sst I plus Sal I, respectively; lanes 3 and 4, HTLV-Ib (λMC) DNA digested with Sst I plus Pst I and Sst I plus Sal I, respectively; lanes 5 and 6, HTLV-II (pMO) DNA digested with Bam HI plus Xho I and Bam HI plus Eco RI, respectively. HTLV-I (λST) and HTLV-I (λMC) clones were obtained from the genomic libraries of DNA's from ATL patients S.T. and M.C., respectively. Both cellular DNA's were cloned at the Sst I site of phage λgtWES · λB DNA (*16*). HTLV-I (λST) is a prototype HTLV-I and HTLV-Ib (λMC) is a variant of HTLV-I that contains some divergent restriction enzyme sites, including the lack of the second Pst I site from the 5′ end of the viral genome (*16*). HTLV-II (pMO) was obtained by subcloning λMO15A (*26*) at the Bam HI site of plasmid pBR322 DNA. The cDNA was synthesized as described in Fig. 1 and hybridization was performed at 37°C for 16 hours in a mixture containing 30 percent formamide, 5× SSC, 5× PM, denatured DNA (100 μg/ml), 0.1 percent SDS, and 10 percent dextran sulfate. The membrane was subsequently washed and exposed as described in Fig. 1.

legend to Fig. 2 and blot-hybridized to ^{32}P-labeled HTLV-III$_B$ cDNA. A region spanning the *gag* and *pol* genes showed the greatest homology. For the prototype HTLV-I, this corresponds to the 1.7-kb Pst I–Pst I fragment and 5.3-kb Sst I–Sal I fragment. HTLV-Ib, which lacks a Pst I site indicated in parentheses in Fig. 2, revealed the expected 3.0-kb Pst I–Pst I fragment instead. Similarly, strong hybridization to the *gag-pol* sequences of HTLV-II also occurred. This is reflected in the 4.2-kb Bam HI–Xho I fragment and the 4.0-kb Bam HI–Eco RI fragment (Fig. 2, lanes 5 and 6).

Fragments corresponding to the *env* and pX sequences of HTLV-I and HTLV-II also hybridized weakly with HTLV-III$_B$ cDNA (see the 2.4-kb Pst I–Pst I and the 2.1-kb Sst I–Pst I fragment in Fig. 2, lane 1) as did the 1.4-kb Pst I fragment of HTLV-Ib containing only pX sequences (Fig. 2, lane 4). The ease of detection of these sequences varied with different preparations of cDNA, probably because of variable representations of the 3′ end of the virus genome. We used cDNA from both HTLV-III$_B$ and HTLV-III$_Z$. Figure 3 shows the results for HTLV-III$_Z$ cDNA. Subclones of HTLV-I containing different regions of the genome were hybridized to HTLV-III$_Z$ cDNA (Fig. 3A). With the exception of fragment c, which corresponds to an internal portion of the *pol* gene, all fragments were detected by hybridization, including fragment a (LTR-*gag*) after long exposure of the autoradiogram. Similarly, the 3′ half of HTLV-II contained in the 3.5-kb Bam HI–Bam HI fragment and the 2.3-kb Bam HI–Xho I fragment could be detected with this particular HTLV-III cDNA probe (Fig. 3B).

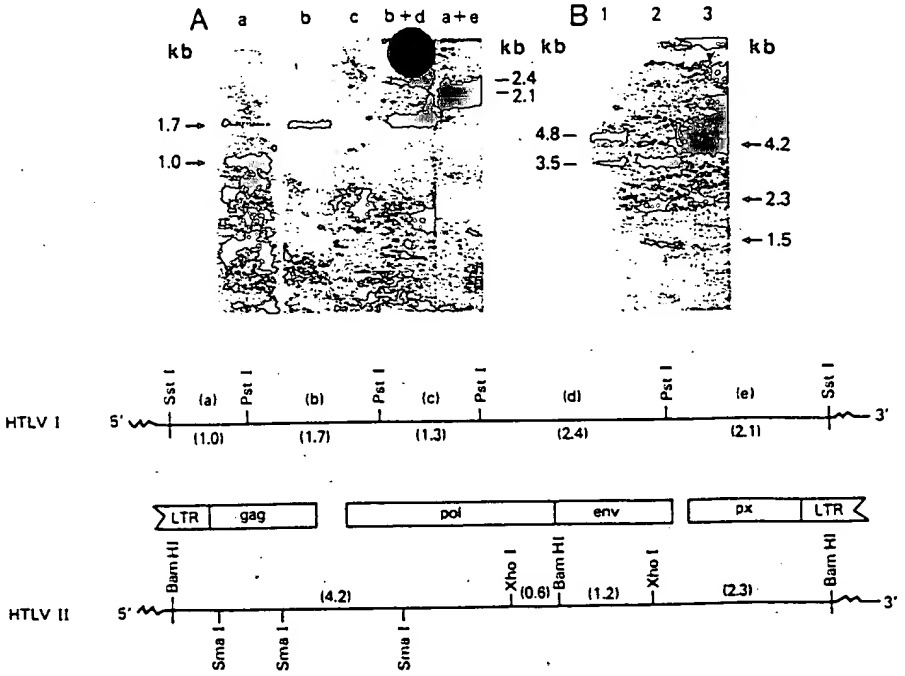

Fig. 3. Relatedness of the genome of HTLV-III$_Z$ with the genomes of HTLV-I and HTLV-II. DNA from subclones of HTLV-I$_{ST}$ and HTLV-II$_{MO}$ was digested with the indicated restriction enzymes. Fragments were separated by agarose gel electrophoresis, transferred to a nitrocellulose membrane (*24*), and hybridized with HTLV-III$_Z$ cDNA. (A) HTLV-I subclones were constructed by "shotgun" cloning of fragments generated by codigestion with Pst I and Sst I into pBR322 containing fragments designated a to e on the illustrated restriction map of HTLV-I. The viral inserts were released by digestion with the appropriate enzymes. (B) HTLV-II (pMO) DNA: Lane 1, digested with Bam HI; lane 2, digested with Bam HI plus Sma I; lane 3, digested with Bam HI plus Xho I. The cDNA was synthesized as in Fig. 1 and hybridization was performed as in Fig. 2, except that the hybridization mixture contained 40 percent formamide.

Retroviruses called LAV (or sometimes IDAV$_1$ and IDAV$_2$) have been isolated from patients with lymphadenopathy syndrome and AIDS (*17*). Although LAV has been reported to lack relatedness to HTLV-I and -II (*17*), further characterization of its proteins and nucleic acids may reveal that LAV is related to these viruses and is identical to or related to HTLV-III.

The present data showing that certain nucleotide sequences of HTLV-III are homologous to sequences of HTLV-I and HTLV-II support our proposal that this virus should be classified within the HTLV family. However, HTLV-III is much less related to HTLV-II and HTLV-I than HTLV-II and HTLV-I are to each other. It is of interest that still other HTLV-related T lymphotropic retroviruses have been identified in Old World monkeys (*18*). These primate viruses are closely related to HTLV-I and only minimally to HTLV-II (*19*). Although the most conserved sequences of HTLV-III are in the region spanning the junction of the predicted *gag* and *pol* genes, other weakly homologous sequences are also detected in the *env* and pX genes. Homology in the *gag* and *env* coding sequences has already been suggested by immunological cross-reactivity between these antigens derived from the three subgroups (*14*). Homology in the pX region is an additional demonstration that HTLV-III belongs to the HTLV family, which is unique among retroviruses in its possession of the pX genes (*20*, *21*). It is interesting that pX is the most conserved region between HTLV-I and HTLV-II (*21*) and that both of these viruses can transform T cells in vitro. In contrast, the pX region is much less conserved in HTLV-III, a cytopathic virus that lacks transforming activity (*11*, *12*).

Comparisons of the LTR regions between HTLV-I and HTLV-II have revealed a conserved 21-bp repeat sequence in two otherwise very divergent LTR's (*22*). The location of this sequence upstream of promoter sequences suggests that it is similar to other viral enhancer sequences. In view of the tropism of HTLV-III for OKT4$^-$ lymphocytes, it will be interesting to see if this virus also has such an enhancer sequence in its LTR. Our present study does not allow us to compare specifically the LTR of HTLV-III to those of HTLV-I and -II. However, the weak signal obtained with 5′ and 3′ ultimate fragments containing the LTR suggest that these elements have minimal or no homology.

SURESH K. ARYA
ROBERT C. GALLO
BEATRICE H. HAHN
GEORGE M. SHAW
MIKULAS POPOVIC
S. ZAKI SALAHUDDIN
FLOSSIE WONG-STAAL

Laboratory of Tumor Cell Biology, Developmental Therapeutics Program, Division of Cancer Treatment, National Cancer Institute, Bethesda, Maryland 20205

References and Notes

1. R. C. Gallo and F. Wong-Staal, *Blood* 60, 545 (1982); R. C. Gallo, in *Cancer Surveys*, L. M. Franks, L. M. Wyke, R. A. Weiss, Eds. (Oxford Univ. Press, Oxford, 1984), vol. 3, pp. 113–159.
2. V. S. Kalyanaraman *et al.*, *Science* 218, 571 (1982).
3. I. Miyoshi *et al.*, *Nature (London)* 294, 770 (1981); M. Popovic, G. Lange-Wantzin, P. S. Sarin, D. Mann, R. C. Gallo, *Proc. Natl. Acad. Sci. U.S.A.* 80, 5402 (1983); P. D. Markham *et al.*, *Int. J. Cancer* 31, 413 (1983); I. S. Y. Chen

et al., *Nature (London)* 305, 502 (1983); M. Popovic *et al.*, in *Human T-Cell Leukemia Viruses*, R. C. Gallo, M. Essex, L. Gross, Eds. (Cold Spring Harbor Laboratory, Cold Spring Harbor, N.Y., in press).
4. M. Popovic *et al.*, in preparation.
5. M. Popovic, F. Wong-Staal, P. S. Sarin, R. C. Gallo, *Adv. Viral Oncol.* 4, 45 (1984); K. Nagy, P. Clapham, R. Cheingson-Popov, R. A. Weiss, *Int. J. Cancer* 32, 321 (1983).
6. H. Mitsuya *et al.*, *Science* 223, 1293 (1984).
7. Centers for Disease Control Task Force on Kaposi's Sarcoma and Opportunistic Infections, *N. Engl. J. Med.* 306, 248 (1982); J. P. Hanrahan, G. P. Wormser, C. P. Macquire, L. J. DeLorenzo, G. Davis, *ibid.* 307, 498 (1982); J. W. Curran *et al.*, *ibid.* 310, 69 (1984).
8. R. C. Gallo, P. S. Sarin, W. A. Blattner, F. Wong-Staal, M. Popovic, in *Seminars in Oncology: AIDS*, J. E. Groopman, Ed. (Grune & Stratton, San Diego, 1984), pp. 12–17; M. Essex *et al.*, in *Human T-Cell Leukemia Viruses*, R. C. Gallo, M. Essex, L. Gross, Eds. (Cold Spring Harbor Laboratory, Cold Spring Harbor, N.Y., in press).
9. M. Essex *et al.*, *Science* 220, 859 (1983); *ibid.* 221, 1061 (1983); T. H. Lee *et al.*, *Proc. Natl. Acad. Sci. U.S.A.*, in press.
10. R. C. Gallo *et al.*, *Science* 220, 865 (1983); B. H. Hahn *et al.*, in *Acquired Immune Deficiency Syndrome. UCLA Symposia on Molecular and Cellular Biology*, M. S. Gottlieb and J. E. Groopman, Eds. (Liss, New York, in press).
11. R. C. Gallo *et al.*, *Science* 224, 500 (1984).
12. M. Popovic, M. G. Sarngadharan, E. Read, R. C. Gallo, *ibid.*, p. 497.
13. M. G. Sarngadharan, M. Popovic, L. Bruch, J. Schupbach, R. C. Gallo, *ibid.*, p. 506; M. G. Sarngadharan *et al.*, in preparation.
14. J. Schüpbach *et al.*, *Science* 224, 503 (1984).
15. G. Franchini, F. Wong-Staal, R. C. Gallo, *Proc. Natl. Acad. Sci. U.S.A.*, in press.
16. B. Hahn *et al.*, *Int. J. Cancer*, in press.
17. F. Barre-Sinoussi *et al.*, *Science* 220, 868 (1983); E. Vilmer *et al.*, *Lancet* 1984-I, 753 (1984); L. Montagnier, personal communication.
18. I. Miyoshi *et al.*, *Gann* 74, 323 (1983); C. W. Saxinger *et al.*, in *Human T-Cell Leukemia Viruses*, R. C. Gallo, M. Essex, L. Gross, Eds. (Cold Spring Harbor Laboratory, Cold Spring Harbor, N.Y., in press).
19. H.-G. Guo, F. Wong-Staal, R. C. Gallo, *Science* 223, 1195 (1984).
20. M. Seiki, S. Hattori, Y. Hirayama, M. Yoshida, *Proc. Natl. Acad. Sci. U.S.A.* 80, 3618 (1983).
21. G. M. Shaw *et al.*, *ibid.* 81, 4544 (1984).
22. J. Sodroski *et al.*, *ibid.*, in press.
23. E. M. Southern, *J. Mol. Biol.* 98, 503 (1973).
24. R. A. Cox, *Methods Enzymol.* 12, 120 (1967); S. L. Adams *et al.*, *Proc. Natl. Acad. Sci. U.S.A.* 74, 3399 (1980).
25. T. Maniatis, E. F. Fritsch, J. Sambrook, *Molecular Cloning. A Laboratory Manual* (Cold Spring Harbor Laboratory, Cold Spring Harbor, N.Y., 1983), pp. 23–233.
26. E. P. Gelmann *et al.*, *Proc. Natl. Acad. Sci. U.S.A.* 81, 993 (1984).
27. We gratefully acknowledge the help and advice of Dr. P. Markham and the expert editorial assistance of A. Mozzuca.

1 May 1984; accepted 30 May 1984

Growth Self-Incitement in Murine Melanoma B16: A Phenomenological Model

Abstract. *The growing murine melanoma B16 secretes increasing quantities of a substance or substances immunologically cross-reactive with insulin. The elevated concentrations of these substances in blood are accompanied by a decrease in blood glucose concentration and release of growth hormone, which is followed by increased tumor growth. By use of a phenomenological model based on these data, we show that B16 incites its own growth by positive feedback.*

Certain human (*1–5*) and murine (*6–8*) tumors produce and secrete a substance or substances immunologically cross-reactive with insulin (SICRI's). Several features distinguish SICRI's from insulin and show that they are of tumor origin: (i) their high concentrations observed also in tumor-bearing diabetic patients (*2*, *5*) and diabetic mice (*6–9*); (ii) the restoration of normal insulin concentrations after removal of the tumor (*1*, *2*, *4*); (iii) the high concentrations of SICRI's within tumor tissue (*1*, *2*, *9*, *10*); and (iv) the lack of a correlation between concentrations of circulating SICRI's and C-peptide (*5*, *11*). Yet SICRI's display insulin-like action in that they decrease blood glucose in tumor patients (*2–5*) and tumorous mice (*6*, *8*, *9*).

We now show that in murine melanoma B16 the concentration of SICRI's in blood is a function of tumor volume and that glucose concentration in blood is a function of SICRI concentration. The decreased amount of glucose in blood is correlated with elevated amounts of circulating growth hormone which, in turn, is paralleled by increased tumor growth. By use of a phenomenological model based only on correlations of tumor volumes and SICRI and glucose concentrations in blood, we show that a positive feedback—that is, growth self-incitement—occurs in melanoma B16.

Male C57BL/H Irb mice 2.5 months of age and weighing 22 g each were housed five to a cage and given free access to water and standard pelleted food. The tumor, originally obtained from the Holt Radium Institute (Manchester, England), has been maintained at the Rugjer Bošković Institute since 1975 by subcutaneous inoculations of 2×10^6 cells into the flanks of recipient animals. Three opposite diameters (*A*, *B*, and *C*) of almost spherical prolate ellipsoid tumors were measured, and their volume was calculated as $V = ABC\pi/6$. Blood glucose concentrations were measured by the ortho-toluidine method (*12*). The SICRI concentrations were determined by insulin-specific radioimmunoassay (*13*) with the use of Phadebas kits (Uppsala, Sweden); therefore, these concentrations are relative and expressed as insulin equivalents (*5*).

Secreting tumors release SICRI's even in alloxan-diabetic mice (*6*). In normoinsulinemic animals with melanoma B16, SICRI concentrations in the blood may be more than five times greater than normal insulin concentrations and are correlated with tumor volume (Fig. 1A); SICRI's also appear in diabetic melanoma-bearing mice (*9*). By fractionating tumor extract on a Sepharose 6B column, we obtained an apparent relative molecular size for B16 SICRI of 120,000 (*10*), as in non-Hodgkin's lymphoma (*5*). Increase of tumor volume and of SICRI concentrations was accompanied by a decrease in blood glucose concentration (Fig. 1B). The correlation between amounts of SICRI and blood glucose was high.

Our phenomenological model is based on consideration of (i) exponential volume-SICRI and SICRI-glucose relations (Fig. 1) and (ii) the Gompertzian tumor growth model (*14*) modified to include positive feedback and chosen empirically because of its demonstrated applicability to tumor growth (*14*). Figure 2 shows the proposed feedback loop formulated by the following relations.

$$S = ae^{\alpha V};\ a,\alpha > 0 \tag{1}$$

$$G = be^{-\beta S} = be^{-a\beta e^{\alpha V}} = g(V);\ b,\beta > 0 \tag{2}$$

$$V = f(G,t) = V_0\, e^{P_n(G)(1 - e^{-\gamma t})};\ V_0, \gamma > 0 \tag{3}$$

$$P_n(G) = a_1 + a_2G + \ldots + a_nG^{n-1} \tag{4}$$

where S and G denote SICRI and glucose concentrations, respectively, V_0 the initial tumor volume, and V the tumor volume at time (t) after transplantation of the tumor. The symbols a, b, α, β, γ, a_1, a_2, . . . , a_n are parameters obtained by the least-square fitting of the empirically chosen functions 1 to 3 to the data (see Table 1). The parameter a_2 differs significantly from zero, while a_3 (and also a_4, a_5, . . . , a_n) can with fair confidence be taken as zero according to the value of F [see (*15*)]. Thus, volume appears to depend significantly on glucose concentration; this dependence is described by a simple exponential function.

The feedback can be measured by calculating the open-loop gain parameter (Ω) [see (*16*)]. Here the infinitesimal changes of tumor volume (dV) and glucose concentration (dG) according to Eqs. 2 and 3 are

$$dV = \left.\frac{\partial f(x,t)}{\partial x}\right|_{x=G} dG + \left.\frac{\partial f(G,y)}{\partial y}\right|_{y=t} dt \tag{5}$$

$$dG = \left.\frac{\partial g(z)}{\partial z}\right|_{z=V} dV \tag{6}$$

SCIENCE

AMERICAN ASSOCIATION FOR THE ADVANCEMENT OF SCIENCE